

Synthesis, characterization, and application of NiFe/LDH in the removal of Congo Red dye

Larissa Q. Farias^{a,*}, Danilo H. S. Santos^a, Luiz D. Silva Neto^b, Lucas Meili^a

^a Technology Center of Federal University of Alagoas, Av. Lourival Melo Mota, s/n, Maceió-AL, 57072-970, Brazil

^b Polytechnic School, Federal University of Bahia, Rua Professor Aristides Novis 02, Salvador-BA, 40210-630, Brazil

Abstract

Given the need for simplified and efficient technologies to treat contaminated waters, this study explored Layered double hydroxide (LDH) as a low-cost alternative for removing Congo red dye (CR) from synthetic effluents through adsorption. The study investigated the influence of temperature, initial dye concentration, and LDH mass through a 2³ experimental design with a central point. The results indicated that the removal efficiency was significantly affected by the variables' mass and initial concentration. The Freundlich, Langmuir, and Sips isotherms were used to model the adsorption capacity as a function of the equilibrium concentration, and the Sips isotherm presented the best fit for the adsorption of Congo red for all temperatures studied. LDH proved efficient, reaching an adsorption capacity of 55.67 mg g⁻¹, standing out as a potential adsorbent material.

Keywords: Layered material; adsorption; experimental design.

1. Introduction

The increase in industrial activities has resulted in the discharge of large quantities of highly contaminated wastewater [1]. Most of the pollutants are non-biodegradable, have a complex structure, and are chemically stable, which makes their removal by conventional treatment methods more difficult [2–3]. In this sense, the adsorption process has been considered an economically viable and highly effective approach due to its simple operation, low cost, and high efficiency [4]. LDH has recently been highlighted for its exceptional properties in mitigating environmental problems, especially in efficiently removing pollutants from wastewater. This is due to its unique structure of two-dimensional (2D) nanostructured anionic clays, which provide a high anion exchange and adsorption capacity [5]. Therefore, a Ni and Fe LDH was synthesized in this study to evaluate its efficiency in removing the CR dye.

2. Methodology

2.1 Synthesis

Two solutions were prepared for the coprecipitation method. Solution A was an alkaline solution containing 8 g of sodium hydroxide and 1.32 g of sodium carbonate in 100 mL of deionized water, stirred for 30 minutes. Solution B contained 19.194 g of nickel nitrate and 13.332 g of iron nitrate in 20 mL of deionized water, which was stirred until the salts were fully dissolved. Solution A was then slowly added to Solution B while stirring at 1000 rpm for 8 hours, resulting in a brown paste. This paste was centrifuged and washed several times with deionized water, then dried in an oven at 65 °C for 24 hours.

2.2 Characterization of HDL

X-ray diffraction was performed using a Shimadzu XRD-6000 diffractometer equipped with a Ni filter and a CuK α radiation source ($\lambda = 0.1542$ nm), with a voltage of 30 kV and a current of 30 mA. Data were recorded in the 2θ range from 5° to 80°. FTIR-ATR analyses were conducted using a Shimadzu FTIR PRESTIGE 21 spectrophotometer in the spectral range of 4000 cm⁻¹ to 400 cm⁻¹. The samples were examined under a scanning electron

microscope (Tescan VEGA-3 LMU, Brno, Kohoutovice, Czech Republic).

2.3 Adsorption studies

A central point experimental design was used in the adsorption tests. The three independent variables studied at the lower and upper limits of the experimental range and the central point are presented in Table 1.

Table 1. Codification, variables and levels analyzed in the experimental design.

| Cod. | Variables | Levels | | |
|----------|-------------------------------------|--------|-----|-----|
| | | -1 | 0 | 1 |
| <i>M</i> | Mass (g) | 0.1 | 0.2 | 0.3 |
| <i>C</i> | Concentration (mg L ⁻¹) | 20 | 35 | 50 |
| <i>T</i> | Temperature | 20 | 40 | 60 |

The adsorption capacity ($q_{t,e}$) was defined as the response variable. The residual CR concentration was measured by spectrophotometric analysis. The amount of CR adsorbed at the equilibrium time was calculated using Equation 1.

$$q_{t,e} = \frac{(C_0 - C_{t,e}) \cdot V}{M} \quad (1)$$

where C_0 and $C_{t,e}$ are the initial and equilibrium CR concentrations at time t or equilibrium (mg L⁻¹), respectively; V is the volume of the CR solution (L), and M is the mass of the adsorbent in grams (g).

2.3 Kinetic and equilibrium studies of adsorption

The kinetic data were evaluated using three models: pseudo-first order, pseudo-second order, and Elovich. The equilibrium data were evaluated using Langmuir, Freundlich, and Sips isotherms. The equations used to fit the data are presented in Table 2. The evaluation and selection of the kinetic and equilibrium models that best describe the CR adsorption mechanism were based on the correlation coefficient (R^2).

3. Results

3.1 Characterization

X-ray diffraction analysis revealed (Fig. 1a) that the material presented intense peaks at 2θ values 11.16°, 22.8°, 32.1°, 34.1°, 35.5°, 39°, 47.95°, 59.86°, 61.3° which correspond to the basal planes of (003), (006), (101) (012), (009), (015), (018), (110) and (113). These peaks are characteristic of NiFe/LDH (JCPDS No. 49-188) [6].

Table 2. Equations of kinetic models, isotherm, and thermodynamic parameters.

| Model | Mathematical Expression | Eq. |
|---------------------|---|-----|
| Kinetic model | | |
| Pseudo first order | $q_t = q_e (1 - e^{-k_1 t})$ | 2 |
| Pseudo second order | $q_t = \frac{q_e^2 k_2 t}{1 + q_e k_2 t}$ | 3 |
| Elovich | $q_t = \frac{1}{\beta_E} \ln(\alpha_E \beta_E + t)$ | 4 |
| Isotherm model | | |
| Langmuir | $q_e = \frac{q_{max} K_L C_e}{1 + K_L C_e}$ | 5 |
| Freundlich | $q_e = K_F C_e^{1/n}$ | 6 |
| Sips | $q_e = \frac{q_{max} K_S C_e^{n_s}}{1 + K_S C_e^{n_s}}$ | 7 |

where q_e and q_t are the amount of dye adsorbed by adsorbent (mg g⁻¹) at equilibrium and time t (min), respectively; k_1 and k_2 are the pseudo-first-order (min⁻¹) and pseudo-second-order (g mg⁻¹ min⁻¹) adsorption constant, respectively; α_E (mg g⁻¹ min⁻¹) and β_E are Elovich constants; C_e is the concentration of dye at equilibrium (mg L⁻¹); q_{max} is the maximum adsorption capacity of the adsorbent (mg.g⁻¹); K_L , K_F and K_S are Langmuir (L mg⁻¹), Freundlich (mg g⁻¹ (mg L⁻¹)ⁿ), and Sips (L g⁻¹) constants of their respective models of isotherms; n is the dimensionless constant that represents the adsorption intensity; n_s is the exponent of the Sips isotherm model.

The FTIR spectra of the NiFe/LDH sample (Fig. 1b) show a double peak in the range of 3800–3600 cm⁻¹, related to the O–H stretching vibrations of structural hydroxyl groups and adsorbed water, which may also be related to the M–O bond intercalated with water. In addition, there is a prominent peak in the 2366–2300 cm⁻¹ range, leaving the stretching and angular deformation of the C–C bond. The band located in the range of 1400–1300 cm⁻¹ for NiFe/LDH corresponds to the C–O bonds of CO₃²⁻ present in the LDH interlayer. The bands in the 750–500 cm⁻¹ range may represent metal-oxygen (M–O) stretching vibrations,

bringing Fe–O and Ni–O bond vibrations in NiFe/LDH [7].

The morphologies of the material were investigated using scanning electron microscopy, as shown in Fig. 1c. The NiFe/LDH synthesized by coprecipitation exhibited heterogeneous particle sizes featuring stacked nanosheets [7].

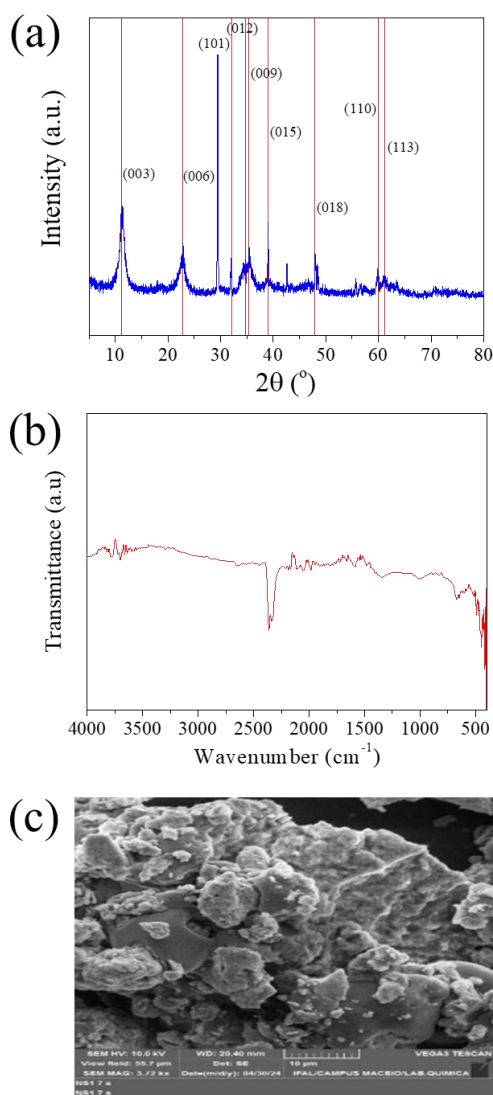


Fig. 1. Characterization of LDH. (a) XDR; (b) FTIR; (c) SEM.

3.2 Adsorption studies

The experimental values found for CR adsorption under the conditions provided by the experimental design show that the adsorption capacity, q , varied

considerably. The lowest value of q , 0.8717 mg g^{-1} , was found at a temperature of 40°C , an initial contaminant concentration of 35 mg L^{-1} and a mass of 0.368 g . The highest value was reached at a temperature of 40°C , an initial contaminant concentration of 35 mg L^{-1} and a mass of 0.032 g , with q equal to 21.7 mg g^{-1} . The Pareto chart used to show the significant variables for response is provided in Fig. 2a.

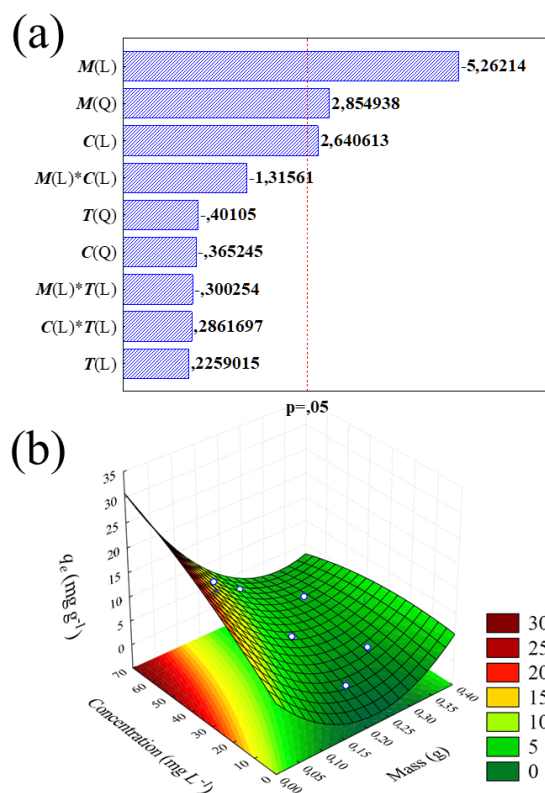


Fig. 2. (a) Pareto and (b) surface graphs.

The positive or negative effect of each factor on the response was marked on the graph as + or – signs, respectively. The graph shows that mass had significant linear and quadratic effects. The effect was linear in the negative direction. The effect of the initial CR concentration was also linearly significant in the positive direction. The synergistic effect of the mass and concentration interaction is presented in Fig. 2b.

3.3 Adsorption kinetics

Fig. 3a presents the kinetic fits of the experimental data. From the parameters obtained in these analyses, it was observed that the data best fit the Elovich model, which is often applied to adsorption systems where the adsorbent surface is heterogeneous, and the adsorption rate decreases with time due to surface coverage. In addition, the equilibrium data indicated a maximum adsorption capacity of 55.67 mg g^{-1} . The equilibrium was represented by the Sips model, which combines features of the Langmuir and Freundlich models, being suitable for describing systems with heterogeneity of adsorption sites at high solutes Fig. 3b [2].

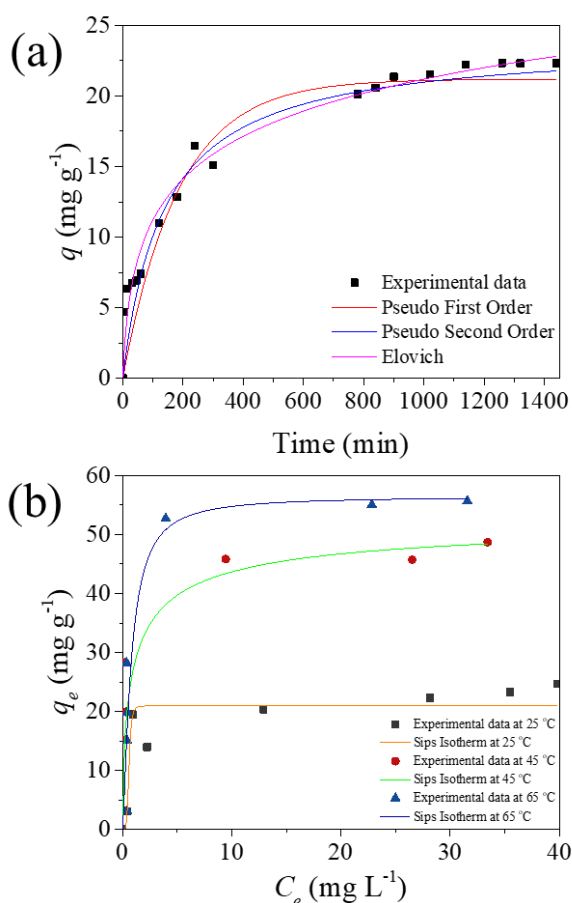


Fig. 3. (a) Kinetics and (b) isotherms of adsorption.

4. Conclusion

Based on the adsorption data obtained in this study, the material demonstrated excellent performance and is considered a promising adsorbent for

removing pollutants such as Congo Red (CR) from aqueous effluents. Its efficiency and adsorption capacity highlight it as a viable option for future applications in contaminated water treatment.

Acknowledgments

I am grateful to the Federal University of Alagoas, CAPES, FAPEAL, the LAPRO process laboratory, partner laboratories, and my advisor, Lucas Meili.

References

- [1] D. Wang et al., "Dual functional sites strategies toward enhanced heavy metal remediation: Interlayer expanded Mg-Al layered double hydroxide by intercalation with L-cysteine," *J Hazard Mater*, vol. 439, p. 129693, Oct. 2022.
- [2] P. S. Jijoe, S. R. Yashas, and H. P. Shivaraju, "Fundamentals, synthesis, characterization and environmental applications of layered double hydroxides: a review," *Environ Chem Lett*, vol. 19, no. 3, pp. 2643–2661, Jun. 2021.
- [3] Y. S. Ravindra, S. H. Puttaiah, S. Yadav, and J. S. Prabagar, "Evaluation of polymeric g-C₃N₄ contained nonhierarchical ZnV₂O₆ composite for energy-efficient LED assisted photocatalytic mineralization of organic pollutant," *Journal of Materials Science: Materials in Electronics*, vol. 31, no. 19, pp. 16806–16818, Oct. 2020.
- [4] W. Huang et al., "Surface protection method for the magnetic core using covalent organic framework shells and its application in As(III) depth removal from acid wastewater," *Journal of Environmental Sciences*, vol. 115, pp. 1–9, May 2022.
- [5] J. O. Eniola, R. Kumar, A. A. Al-Rashdi, M. O. Ansari, and M. A. Barakat, "Fabrication of Novel Al(OH)₃/CuMnAl-Layered Double Hydroxide for Detoxification of Organic Contaminants from Aqueous Solution," *ACS Omega*, vol. 4, no. 19, pp. 18268–18278, Nov. 2019.
- [6] HUANG, Feng et al. NiFe layered double hydroxide nanosheet arrays for efficient oxygen evolution reaction in alkaline media. *International Journal of Hydrogen Energy*, v. 47, n. 51, p. 21725-21735, 2022.
- [7] Taher, T., Putra, R., Palapa, N. R., & Lesbani, A. (2021). Preparation of magnetite-nanoparticle-decorated NiFe layered double hydroxide and its adsorption performance for congo red dye removal. *Chemical Physics Letters*, 777, 138712.